ISSN 0021-3640, JETP Letters, 2011, Vol. 94, No. 3, pp. 192–196. © Pleiades Publishing, Inc., 2011.
Original Russian Text © S.G. Ovchinnikov, 2011, published in Pis'ma v Zhurnal Eksperimental'noi i Teoreticheskoi Fiziki, 2011, Vol. 94, No. 3, pp. 210–214.

# Metallization and Spin Crossover in Magnesiowüstite ($Mg_{1-x}Fe_xO$) at High Pressures

**S. G. Ovchinnikov**

*Kirensky Institute of Physics, Siberian Branch, Russian Academy of Sciences, Akademgorodok, Krasnoyarsk, 660036 Russia*

*Siberian Federal University, Svobodnyi pr. 79, Krasnoyarsk, 660041 Russia*

*e-mail: sgo@iph.krasn.ru*

Received May 27, 2011

The pressure–temperature phase diagram of magnesiowüstite has been constructed using the many-electron LDA+GTB approach. The phase diagram includes a quantum critical point at $P_c = 55$ GPa and has a symmetrical distribution of high-spin and low-spin states. The existence of a metallic state in a narrow temperature range above the critical point is predicted.

**DOI:** 10.1134/S0021364011150094

## 1. INTRODUCTION

Magnesiowüstite ($Mg_{1-x}Fe_xO$) is a mineral with the NaCl (fcc) structure. In the lower Earth's mantle, its content is about 30%. Therefore, the properties of (Mg,Fe)O solid solutions at high pressures are of interest for both condensed matter physics and geophysics. The spin crossover of $Fe^{2+}$ ions from the high-spin (HS) state with spin $S = 2$ to the low-spin (LS) state with spin $S = 0$ was observed in the high-pressure experiments with the use of diamond anvil cells [1, 2]. The features of the spin crossover are currently under discussion. The data reported in [3] suggest that the spin-state transition is smeared within the 50–100 GPa range, whereas in [2], this range turns out to be narrower (62–6 GPa).

The later more careful measurements of the usual Mössbauer and synchrotron X-ray diffraction spectra of $Mg_{0.75}Fe_{0.25}O$ [4] demonstrate that this crossover at room temperature occurs within the 55–70-GPa pressure range. Similar low-temperature studies at 8 K < $T$ < 300 K revealed that the transition range becomes narrower upon cooling. Using these data, Lyubutin et al. [5] concluded that there is a quantum critical point $P_c$ at zero temperature, where the HS–LS transition occurs in a stepwise manner. In this work, the electronic and magnetic properties of magnesiowüstite are treated theoretically in the framework of the many-electron theory taking explicitly into account the intraatomic Coulomb interactions [6]. Only the case of $Mg_{1-x}Fe_xO$ with the iron content exceeding the percolation threshold (for $x = 0.25$, this condition is certainly satisfied) is considered. In this case, the long-range magnetic order or metallic conductivity in FeO leads to the similar properties of magnesiowüstite. The properties of FeO and $Mg_{0.75}Fe_{0.25}O$ are alike in many respects, but there are some differences. For example, they have the same structure of their fcc lattice and there is a long-range antiferromagnetic order with $T_N = 25$ K in $Mg_{0.75}Fe_{0.25}O$ [7] and $T_N = 198$ K in FeO. In FeO, the spin crossover has not been observed. Up to 143 GPa, it retains the HS state (according to the X-ray photoemission spectroscopy data) [8]. The metallization of FeO was observed at $P > 140$ GPa [9], whereas the measurements of the conductivity for $Mg_{0.75}Fe_{0.25}O$ both in the HS and LS states at pressures up 101 GPa reveal only a semiconducting behavior with a slight increase in the conductivity at $P \approx 50$ GPa [10]. Despite the common approach to the description of the electronic structure in FeO and $Mg_{0.75}Fe_{0.25}O$ and the same values of intraatomic Coulomb matrix elements, the crystal field splitting $10Dq$ has different values in these substances. Wüstite FeO is a classical example of the Mott–Hubbard insulators. Its properties are determined by the strong electron correlations [11]. With increasing pressure, the band gap $E_g$ decreases due to an increase in the bandwidth $2W$ and, at $P = P_{MIT}$, the transition to a metallic phase is expected. In addition, the magnetic insulators can exhibit a spin crossover at point $P_c$ corresponding to the transition of the magnetic ion from the HS to LS state [12]. For the compounds with $d^5$ ions, the spin crossover favors the metallization due to the decrease in the effective Hubbard parameter $U_{eff} = E_0(d^{n+1}) + E_0(d^{n-1}) - 2E_0(d^n)$, where $E_0(d^n)$ is the energy corresponding to the ground-state term of a $d^n$ ion [13]. However, for the $d^6$ ion, as was shown in [13], the spin crossover leads to an increase in $U_{eff}$. In this work, it is demonstrated that this fact gives rise to a quite unusual phase diagram for magnesiowüstite, where the metal-

lic state can exist within a narrow pressure range above $P_c$ and only at nonzero temperatures.

The band structure calculations for FeO by the LDA+DMFT method [14] taking into account strong electron correlations lead to the prediction of the transition to a metallic state at $P_{\mathrm{MIT}} = 60$ GPa. In a large number of oxides with iron ions, the critical pressure $P_c$ falls within the same pressure range, $P_c = 55$–70 GPa [12]. The close proximity (and, in fact, the coincidence accurate up to an experimental error) of two critical pressures, $P_{\mathrm{MIT}}$ and $P_c$, determines the specific features of the phase diagram for $Mg_{0.75}Fe_{0.25}O$.

## 2. SPIN AND CHARGE EXCITATIONS IN THE MANY-ELECTRON THEORY

The hybrid LDA+GTB method was initially formulated for the description of the band structure of high-$T_c$ superconductors [15]. It combines the LDA calculations of the parameters involved in the multiband Hubbard model with the many-electron approach provided by the generalized tight binding (GTB) technique. In essence, the GTB method is a version of cluster-type perturbation theory, where, at the first stage, the exact diagonalization of the Hamiltonian within a single unit cell is performed and, at the second stage, the intercell hopping is described according to perturbation theory [16]. In the case under study, the unit cell corresponds to the $FeO_6$ cluster. According to the electroneutrality condition for FeO, the $Fe^{2+}$ ion has the $d^6$ configuration. The problem of finding eigenstates for a $d^6$ ion in the crystal field of cubic symmetry with the complete inclusion of all matrix elements has been solved long ago [17]; its generalization including the effects of covalence and spin-orbit interaction was reported in [18].

The energies of the terms that will be needed below are as follows. For the high-spin states,

$$\begin{aligned} E_{\mathrm{HS}} \equiv E(d^6, {}^5T_2) &= 6\varepsilon_d + 15A - 35B + 7C - 4Dq, \\ E(d^7, {}^4T_1) &= 7\varepsilon_d + 21A - 40B + 14C - 8Dq, \\ E(d^5, {}^6A_1) &= 5\varepsilon_d + 10A - 35B. \end{aligned} \quad (1)$$

Here, $\varepsilon_d$ is the energy of the atomic $d$ level and $A$, $B$, and $C$ are the Racah parameters. For the low-spin states,

$$\begin{aligned} E_{\mathrm{LS}} \equiv E(d^6, {}^1A_1) &= 6\varepsilon_d + 15A - 30B + 15C - 24Dq, \\ E(d^7, {}^2E) &= 7\varepsilon_d + 21A - 36B + 18C - 18Dq, \\ E(d^5, {}^2T_2) &= 5\varepsilon_d + 10A - 20B + 10C - 20Dq. \end{aligned} \quad (2)$$

The ground state of the whole crystal in the stoichiometric case is characterized by the HS state of $Fe^{2+}$ ions at each lattice site. In addition to the usual fluctuations of spin directions, the energy of the spin fluctuations of between HS and LS states is important for this study. This energy is referred to as the spin gap

$$\varepsilon_s = E_{\mathrm{HS}} - E_{\mathrm{LS}} = 20Dq - 5B - 8C. \quad (3)$$

We assume that the Racah parameters are independent of the pressure, while the crystal-field splitting increases linearly with the pressure, $10Dq(P) = 10Dq(0) + \alpha_\Delta P$. Then, the pressure dependence of the spin gap has the form

$$\begin{aligned} \varepsilon_s(P) &= \varepsilon_s(0) + 2\alpha_\Delta P, \\ \varepsilon_s(0) &= 20Dq(0) - 5B - 8C. \end{aligned} \quad (4)$$

In the absence of the applied pressure, the HS state exists; hence, $\varepsilon_s < 0$. However, the growth of pressure can lead to the spin-state transition from the HS to LS state if the pressure achieves a critical value

$$P_c = [2.5B + 4C - 10Dq(0)]/\alpha_\Delta. \quad (5)$$

Two types of charge excitations are possible in the HS state, i.e., with the creation of an electron (excitation $d^6\,({}^5T_2) \longrightarrow d^7\,({}^4T_1)$) and with the creation of a hole (excitation $d^6\,({}^5T_2) \longrightarrow d^5\,({}^6A_1)$). The former and latter determine the upper ($\Omega_+$(HS)) and lower ($\Omega_-$(HS)) Hubbard bands, respectively.

The corresponding energies are

$$\begin{aligned} \Omega_+(\mathrm{HS}) &= \varepsilon_d + 6A - 5B + 7C - 4Dq, \\ \Omega_-(\mathrm{HS}) &= \varepsilon_d + 5A + 7C - 4Dq. \end{aligned} \quad (6)$$

Their difference (the excitation from the lower Hubbard band to the upper one) determines the effective Hubbard parameter, which is independent of the pressure

$$\begin{aligned} U_{\mathrm{eff}}(\mathrm{HS}) &\equiv E(d^7, {}^4T_1) + E(d^5, {}^6A_1) \\ &- 2E(d^6, {}^5T_2) = A - 5B. \end{aligned} \quad (7)$$

Similarly, for the low-spin states,

$$\begin{aligned} \Omega_+(\mathrm{LS}) &= \varepsilon_d + 6A - 6B + 3C + 6Dq, \\ \Omega_-(\mathrm{LS}) &= \varepsilon_d + 5A - 10B + 5C - 4Dq. \end{aligned} \quad (8)$$

In the low-spin state, the parameter

$$U_{\mathrm{eff}}(\mathrm{LS}) = A + 4B - 2C + 10Dq \quad (9)$$

increases with pressure. This result was obtained previously in [13] using another method.

As in the usual tight binding method, interatomic hopping with amplitude $t_{ij}$ between cells $\mathbf{R}_i$ and $\mathbf{R}_j$ leads to the dispersion of the energies of the Hubbard fermions given by Eqs. (6) and (8) and to the formation of the band structure. These calculations require the introduction of the Hubbard $X$ operators and the determination of the electron Green's function according to perturbation theory [19–21]. Using the simplest Hubbard I type approximation for the inter-

atomic hopping, the dispersion law for the $m$th band can be written in the form

$$\Omega_m(k) = \Omega_m + F_m t(k), \quad (10)$$

where subscript $m$ has one of four possible values (HS/LS, +/−), $t(k)$ is the Fourier transform of the hopping amplitude $t_{ij}$, and the filling factor $F_m$ equals the sum of the occupation numbers of the initial and final states involved in the $m$th excitation. In the stoichiometric case, when the $d^5$ and $d^7$ states are not occupied, and the $d^6$ state is occupied with the probability $n_{\rm HS}$ and $n_{\rm LS} = 1 - n_{\rm HS}$ for HS and LS states, respectively,

$$F_{\rm HS} = n_{\rm HS}, \quad F_{\rm LS} = n_{\rm LS}. \quad (11)$$

The dependence of the band energy on the occupation numbers is one of the effects related to strong electron correlations. Another effect manifests itself in the spectral weight of each quasiparticle (a residue of the corresponding Green's function), which is determined by the same filling factor $F_m$.

According to [14], FeO is a Mott–Hubbard insulator; hence, the filled valence oxygen $p$ band can be disregarded. Then, the band gap in the HS state is

$$E_g = U_{\rm eff}({\rm HS}) - 2F_{\rm HS}W. \quad (12)$$

The half-width of the band $W = zt$ (where $z$ is the number of the nearest neighbors; for the fcc lattice, $z = 12$) depends on the pressure via the hopping integral $t$. As a result, the band gap decreases with the growth in $P$ as follows:

$$E_g(P) = E_g(0) - \alpha_W P, \quad \alpha_W = \partial W/\partial P. \quad (13)$$

The critical pressure for the insulator–metal transition is $P_{\rm MIT} = E_g(0)/\alpha_W$. In a more rigorous theory, e.g., in the dynamic mean field approximation, $P_{\rm MIT}$ is numerically different from that given by the Hubbard I approximation. Nevertheless, in this case, $U_{\rm eff}/W(P_{\rm MIT}) \sim 1$ is also valid; that is, there is no quantitative difference. In this work, it is important to demonstrate the possibility of the metallization in principle. The $P_{\rm MIT}$ value was taken from the LDA+DMFT calculations for FeO [14].

Thus, there exist two critical parameters related to the growth of pressure: charge gap (13) vanishing at $P_{\rm MIT}$ and spin gap (4) vanishing at $P_c$. At $P_{\rm MIT} \ll P_c$, the metallization will occur at the stable HS background; just this result was obtained in [14]. At $P_{\rm MIT} \gg P_c$, the spin crossover to the LS state will occur in the insulating phase. As was mentioned in the Introduction, $P_{\rm MIT} \approx P_c$ is characteristic of $Mg_{0.75}Fe_{0.25}O$.

## 3. PHASE DIAGRAM OF MAGNESIOWÜSTITE

At arbitrary values of $P$ and $T$, the probability of finding the $Fe^{2+}$ ion in the HS state is

$$n_{\rm HS} = g_{\rm HS}e^{-\beta E_{\rm HS}}/(g_{\rm HS}e^{-\beta E_{\rm HS}} + g_{\rm LS}e^{-\beta E_{\rm LS}}) = 1/\left(1 + \frac{g_{\rm LS}}{g_{\rm HS}}e^{+\beta\varepsilon_s}\right). \quad (14)$$

Here, $\beta = 1/kT$. The degeneracy orders for the terms under study are $g_{\rm LS} = 1$ and $g_{\rm HS} = (2S + 1)(2L + 1) = 15$. The Racah parameters, $A = 2$ eV, $B = 0.084$ eV, and $C = 0.39$ eV, are obtained for $Fe^{3+}$ in $FeBO_3$ ferroborate by the comparison with the optical data [22]. These values are also assumed for $Fe^{2+}$. For magnesiowüstite, the crystal field splitting is $10Dq(0) = 1.34$ eV [23]. Based on condition (5) at $P_c = 56$ GPa, $\alpha_\Delta = 0.007$ eV/GPa is obtained.

The distribution of the portion of the HS states, $n_{\rm HS}(P, T)$ (phase diagram) is shown in Fig. 1. At all nonzero temperatures, the HS–LS transition is a gradual crossover and only at $T = 0$, there is a jump at $P = P_c$. According to [24], there exists a quantum phase transition at the point $(P_c, 0)$. The fluctuations in the vicinity of the critical point are the fluctuations of the absolute value of the spin. The Néel temperature, which is nonzero in the HS state, vanishes at this point [4].

As follows from Eq. (14), the phase diagram can be represented by the $P(T)$ function for given values of $n_{\rm HS}$ and $n_{\rm LS}$ as

$$P = P_c + \frac{kT}{2\alpha_\Delta}\ln\frac{g_{\rm HS}n_{\rm LS}}{g_{\rm LS}n_{\rm HS}}. \quad (15)$$

Note that, if the degeneracy orders are equal, $g_{\rm HS} = g_{\rm LS}$ (e.g., for $Fe^{3+}$ ion) and the phase diagram (15) is symmetric with respect to the vertical line $P = P_c$, where $n_{\rm HS} = n_{\rm LS}$. In the case of $Fe^{2+}$, for which $g_{\rm HS}/g_{\rm LS} = 15$, the phase diagram is characterized by a pronounced asymmetry and the $n_{\rm HS} = n_{\rm LS}$ line in the $(P, T)$ plane is significantly inclined to the right (Fig. 2).

Now, let us discuss the changes in electrical characteristics in the case $P_{\rm MIT} = P_c$. According to Eq. (13), the band gap in the HS state decreases with the growth of $P$ and vanishes at $P = P_{\rm MIT}$. If the spin crossover did not occur at this point, a metallic state would arise at $P > P_{\rm MIT}$. As a result of the spin crossover, $U_{\rm eff}({\rm LS}) > U_{\rm eff}({\rm HS})$ and the gap could arise again. However, the electronic structure in the LS state depends on $P$ and $T$ in a more complicated way. Just after the spin-state transition, at $P > P_c$, the lowest term for the $d^6$ and $d^5$ configurations is the LS and HS states, respectively. Therefore, at $T = 0$, when only the $^1A_1$ term for the $d^6$ configuration is occupied, the creation of a hole occurs in the final $d^5$ state, while the occupation of the $^6A_1$ term is forbidden due to the spin conservation law. Exactly the same scheme of the multielectron levels corresponding to $d^5$, $d^6$, and $d^7$ configurations with $E_{\rm LS} < E_{\rm HS}$ takes place for $LaCoO_3$ in the absence of the

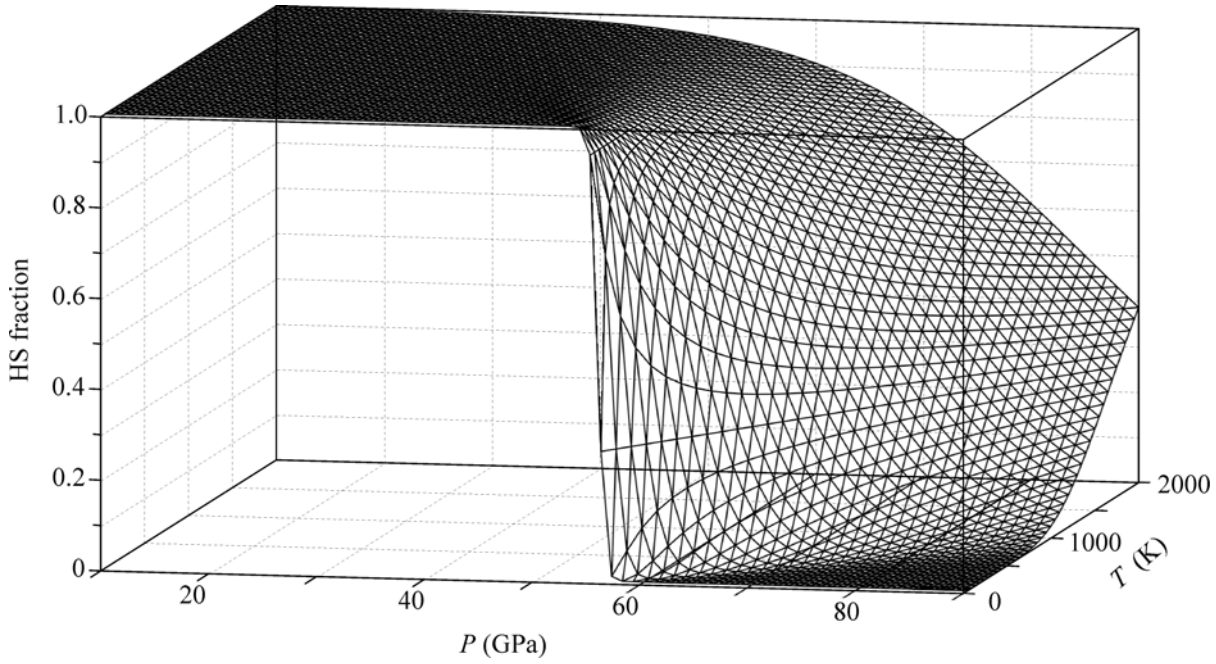


**Fig. 1.** Temperature and pressure distribution of HS states.

applied pressure. The detailed LDA+GTB calculations of the electronic structure for the last compound are reported in [25]. The difference of $LaCoO_3$ from $Mg_{0.75}Fe_{0.25}O$ in the LS state is only in the value of the spin gap. The LS state at $T = 0$ indeed corresponds to an insulator. However, the $d^6$ HS state gradually begins to be occupied at $T \neq 0$ (see Figs. 1 and 2). As a result, it is possible to annihilate an electron in the excited $d^6$ HS state forming the $d^5$ HS final state. This gives rise to a new band of in-gap states with the width and spectral weight that increase proportionally to $n_{HS}$. Thus, the band gap becomes narrower with the growth of the temperature. As follows from the calculations reported in [25], the band gap vanishes at $n_{HS} \approx 0.8$ and metallization takes place. Since the spin gap increases with the pressure, the metal–insulator phase boundary also shifts toward higher pressures (Fig. 2). It is clear that the metallization at a nonzero temperature occurs in the form of a smeared gradual transformation of the semiconductor to metal. Hence all metal–nonmetal phase boundaries in Fig. 2 have this meaning. At $P > P_c$, on the right of the $n_{HS} = 0.8$ line, there is a semiconducting region with the thermal fluctuations involving both the HS and LS states. In Fig. 2, it can be seen that the pressure range corresponding to the metallic state at $T = 300$ K has the width $\Delta P \approx 4$ GPa. This value is of the order of the experimental error for the pressure measurements. Thus, it is not surprising that the authors of [10] concluded that both the HS and LS states have the insulating nature. Nevertheless, they observed a small conductivity peak in the vicinity of $P_c$, which lends an indirect support to our conclusions.

To conclude, note that, in the case of $d^6$ ions, there appears an unusual relation between the spin crossover and metallization. On one hand, the spin crossover leads to the growth of the correlation-induced gap at $T = 0$ and prevents the usual insulator–metal transition related to the band broadening. On the other hand, a nontrivial mechanism underlying the temperature dependence of the band gap and metallization with the growth of the temperature appears in the LS state.

The work was supported by the Division of Physical Sciences, Russian Academy of Sciences (program

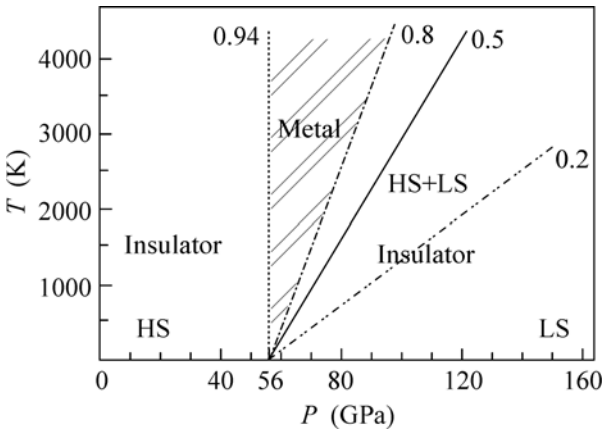


**Fig. 2.** Phase diagram of magnesiowüstite.

"Strong Electron Correlations"), the Siberian and Ural Branches, Russian Academy of Sciences (joint project no. 40), the Russian Foundation for Basic Research (project nos. 09-02-00171 and 10-02-00251), and the Ministry of Education and Sciences (project no. KG P891, federal program "Human Resources"). I am grateful to Yu.S. Orlov, N.V. Lishneva, and I.A. Makarov for their assistance in this work.

## REFERENCES

1. J. Badro, G. Fiquet, F. Guyot, et al., Science **300**, 789 (2003).
2. A. G. Gavrilyuk, J. F. Lin, I. S. Lyubutin, and V. V. Struzhkin, JETP Lett. **84**, 161 (2006).
3. I. Yu. Kantor, L. S. Dubrovinsky, and C. A. McCammon, in *Proceedings of the Joint 20th AIPART and 43rd EHPRG, June 27–July 1, Karlsruhe, Germany, 2005.*
4. I. L. Lyubutin, A. G. Gavrilyuk, K. V. Frolov, et al., JETP Lett. **90**, 617 (2009).
5. I. S. Lyubutin, V. V. Strujkin, A. A. Mironovich, et al., Nature Commun. (in press).
6. S. G. Ovchinnikov, J. Phys.: Condens. Matter **17**, S743 (2005).
7. S. Speziale et al., Proc. Nat. Acad. Sci. USA **102**, 17918 (2005).
8. J. Badro, V. V. Strujkin, J. Shu, et al., Phys. Rev. Lett. **83**, 4101 (1999).
9. V. V. Strujkin, M. I. Eremets, I. M. Eremets, et al., arXiv:1007.4650v1 (2010).
10. J. F. Lin, S. T. Weir, D. D. Jackson, et al., Geophys. Res. Lett. **34**, L16305 (2007).
11. N. F. Mott, *Metal-Insulator Transitions* (Taylor Francis, London, 1974).
12. I. S. Lyubutin and A. G. Gavrilyuk, Phys. Usp. **52**, 989 (2009).
13. S. G. Ovchinnikov, J. Exp. Theor. Phys. **107**, 140 (2008).
14. A. O. Shorikov, Z. V. Pchelkina, V. A. Fybsimov, et al., Phys. Rev. B **82**, 195101 (2010).
15. M. M. Korshunov, V. A. Gavrichkov, S. G. Ovchinnikov, et al., J. Exp. Theor. Phys. **99**, 559 (2004).
16. V. A. Gavrichkov, S. G. Ovchinnikov, A. A. Borisov, and E. G. Goryachev, J. Exp. Theor. Phys. **91**, 369 (2000).
17. Y. Tanabe and S. Sugano, J. Phys. Soc. Jpn. **9**, 753 (1954).
18. Yu. S. Orlov and S. G. Ovchinnikov, J. Exp. Theor. Phys. **109**, 322 (2009).
19. R. O. Zaitsev, *Diagrammatic Methods in the Theory of Superconductivity and Ferromagnetism* (Editorial URSS, Moscow, 2004) [in Russian].
20. A. F. Barabanov, L. A. Maksimov, and A. V. Mikheenkov, Sov. Phys. Solid State **30**, 1449 (1988).
21. S. G. Ovchinnikov and V. V. Val'kov, *Hubbard Operators in the Theory of Strongly Correlated Electrons* (Imperial College Press, London, 2004).
22. I. S. Edel'man and A. V. Malakhovskii, Sov. Phys. Solid State **15**, 2056 (1973).
23. R. G. Burms, *Mineralogical Applications of Crystal Field Theory* (Cambridge Univ. Press, UK, 1993).
24. A. I. Nesterov and S. G. Ovchinnikov, JETP Lett. **90**, 530 (2009).
25. S. G. Ovchinnikov, Yu. S. Orlov, I. A. Nekrasov, and Z. V. Pchelkina, J. Exp. Theor. Phys. **112**, 140 (2011).

*Translated by K. Kugel*